ELSEVIER

Chemical Physics 269 (2001) 389–397

Chemical Physics

www.elsevier.nl/locate/chemphys

The collisional quenching of $CCl_2(A\,^1B_1$ and $a\,^3B_1)$ by substituted methane molecules

Yide Gao, Yang Chen, Xingxiao Ma, Congxiang Chen *

Open Laboratory of Bond Selective Chemistry, Department of Chemical Physics, University of Science and Technology of China, Hefei, Anhui 230026, China

Received 6 March 2001

Abstract

CCl_2 free radical was produced by a pulsed dc discharge of CCl_4 (in Ar). Ground electronic state $CCl_2(X)$ radical was electronically excited to $A\,^1B_1(0,4,0)$ vibronic state with Nd:YAG laser pumped dye laser at 541.52 nm. Experimental quenching data of excited $CCl_2(A\,^1B_1$ and $a\,^3B_1)$ by CH_4, CH_3NO_2, CH_3OH, and halomethanes were obtained by observing time-resolved total fluorescence signal of the excited CCl_2 radical in a cell, which shows a superposition of two exponential decay components under the presence of a quencher. The quenching rate constants K_A of CCl_2 (A) state and K_a of CCl_2 (a) state were derived by analyzing the experimental data according to a proposed three-level model to deal with the $CCl_2(X\,^1A_1, A\,^1B_1, a\,^3B_1)$ system. K_A and K_a increase on the whole with increasing the number of C–Cl bonds in chloromethane molecules. The formation cross sections of complexes between $CCl_2(A\,^1B_1)$ radicals and CH_4, CH_3Cl, CH_3OH and CH_3NO_2 molecules were calculated by means of a collision complex model.

1. Introduction

Since Hine [1] substantiated the original suggestion of Geuther [2] that dichlorocarbene, CCl_2, is involved in the alkaline hydrolysis of chloroform, much effort has gone into the study of the role played by CCl_2 as an intermediate of some organic chemical reactions [3–7]. But, a direct spectroscopic observation of CCl_2 was first carried out in 1967 by Milligan and Jacox using a matrix-isolation technique [8]. CCl_2 radical was often produced by pyrolysis, photolysis, discharge and chemical reaction of some chlorinated hydrocarbon molecules which contain two or more chlorine atoms in same carbon [9–26]. It is found that many industrial processes, such as plasma etching of semiconductor surface [27,28], reprocessing of burnt nuclear fuel [29], relate to CCl_2 radical. Although there has been an extensive study of CCl_2 radical, almost all investigations were focused on the field of spectrum and only a few studies on kinetics of CCl_2 radical have been performed. In 1977 Huie et al. [14] produced CCl_2 radicals through reaction

$$O(^3P) + F_2C{=}CCl_2 \rightarrow F_2CO + CCl_2$$

The radiative lifetimes and quenching rate constants by O_2 were measured for the laser excited CCl_2 at wavelengths 515, 484, 445 and 437 nm, respectively. In 1980 Tiee et al. [17] measured the rate constants of ground state CCl_2 radical reacted with NO, O_2, F_2, CO, C_3H_8, C_2H_4, and

* Corresponding author. Fax: +86-551-3607084.
E-mail address: cxchen@ustc.edu.cn (C. Chen).

0301-0104/01/$ - see front matter
PII: S0301-0104(01)00374-3

Ar. In 1986 Ibuki et al. [20] measured the emission spectrum of excited CCl_2, which were generated by the direct photodecomposition of CCl_4 and $CBrCl_3$ molecules using H Lyman-α or Ar I resonance lines and synchrotron radiation as light sources. The spectra are devoid of structure and show a peak maximum at about 475 nm. They observed the fluorescence decay curve and found that the decay curve is a superposition of two lifetime components, the averaged fast one of 2.17 ± 0.26 μs and slow one of 4.00 ± 0.12 μs, respectively. They measured the quenching rate constants of $CCl_2(A\,^1B_1)$ by CCl_4 and $CBrCl_3$. In 1989 Ibuki et al. [21] generated CCl_2 radical again by the photodecomposition of C_2Cl_6 using synchrotron radiation and obtained the results similar to those in Ref. [20]. In 1996 Wagner [30] generated $CCl_2(X)$ by the reaction

$$C_2O(a) + Cl_2 \rightarrow CCl_2(X) + CO$$

and measured the rate constant of $(7.80 \pm 1.2) \times 10^{-12}$ $cm^3\,molecule^{-1}\,s^{-1}$ for the reaction of the ground state of CCl_2 with Cl_2. Recently, Merelas et al. [26] measured the rate constants for the collisional removal of CCl_2, in its $X\,^1A_1(0,0,0)$ state and $A\,^1B_1(0,7,0)$ electronically excited state by simple alkenes, CH_4, $CF_2{=}CCl_2$, He and Ar at room temperature. We can see from the description aforementioned that, thus far, the investigation of the kinetics of CCl_2 radical, especially for the state-resolved kinetics is insufficient.

In this work, CCl_2 radicals were produced by a pulsed dc discharge of CCl_4 (in Ar) in the discharge cavity and the time-resolved LIF signals of CCl_2 radicals were measured which represent the quenching of the excited CCl_2 radicals by CH_4, CH_3NO_2, CH_3OH, and halomethanes. The state-resolved rate constants K_A and K_a were acquired by analyzing the experimental data according to a proposed three-level model.

2. Experimental section

2.1. Apparatus and method

The dc discharge LIF kinetic experimental setup used in this work consists of a pulsed dc discharge, preparation of gases, reactor, laser source, signal detection, data processing, and time-sequence control system [31].

The dc discharge system is comprised of a high-voltage power source and a discharge cavity. A schematic diagram of the discharge cavity is shown in Fig. 1. Its core part is a polytetrafluoroethylene discharge head with 1 mm gas pathway, which screwed on the movable stainless steel tube. A pair of tungsten pins with a space of 0.5 mm was put into the head perpendicularly to the gas pathway. The pins were fixed onto the discharge head by two screw nails both acting as power terminal and rivet. The power source consists of a silicon controlled rectifier and a pulsed high-voltage transformer with turn ratio of 1:100 and the primary voltage is adjustable. The pulsed dc discharge was initiated between the pair of tungsten needles. The discharge cavity was set at right angle to the laser beam. The distance between the discharge pins and the laser beam was adjusted by moving the stainless steel tube and was 30 mm in this work.

The experiments were performed in a stainless steel reactor by using steady-flow technique. The reactor, preparation of gases and control of flow velocity were described in detail previously [31–34], and only a brief description of modifications for this system is presented here. The parent molecule CCl_4 and the quenching molecules were diluted in a large excess of Ar and stored in 10 l reservoirs prior to experiments. Three gas mixtures were slowly flowing into the reaction vessel: f_1, the

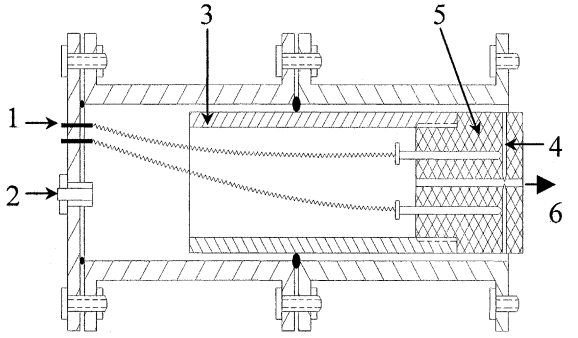

Fig. 1. Schematic framework of discharge cavity: 1. terminal, 2. CCl_4/Ar in, 3. movable stainless steel tube, 4. tungsten needle, 5. discharge head and 6. CCl_2 out.

flow of CCl_4 about 1% in Ar; f_2, the flow of a quenching molecule mixed with Ar; and f_3, the flow of pure Ar. The three flows were measured by mass flow meters (D07-7A/2M, Beijing). The total pressure P_{total} was about 200 Pa and the partial pressure of CCl_4, P_{CCl_4}, in the reaction vessel was about 0.5 Pa. In our experiments, P_{total} and P_{CCl_4} were kept constant. The gases in the vessel were renewed per 0.1 s in order to prevent the results from disturbance of the accumulation of the discharge-produced species and reaction products. The ground electronic state CCl_2 radical was electronically excited to $A\,^1B_1(0,4,0)$ state by a laser beam at 541.52 nm of the dye laser (Lumonics, HD500) pumped by Nd:YAG laser (Spectra physics, GCR-170, repetition rate of 10 Hz). The fluorescence signal of the excited CCl_2 transmitted through a cut-off filter with transmitting wavelengths longer than 580 nm and was detected by a photomultiplier (GDB56, Beijing). The photomultiplier output was recorded by a transient digitizer, and then averaged with a computer data acquisition system. In our experiment the signals were averaged over 1000 laser shots. In order to avoid the mutual disturbing between the laser and discharge system, two photoelectronic isolators were connected between the multi-channel delay generator and the laser, and between the multi-channel delay generator and the discharge system, respectively.

2.1.1. Materials

Ar (99.999%, Nanjing), CF_4 (99.99%, Nanjing), CF_2Cl_2 (99.9%, Nanjing) and CH_4 (99.99%, Chendu) were taken from cylinders without further purification. CH_3Cl, CH_2Cl_2, $CHCl_3$, CCl_4, CH_3NO_2, CH_2Br_2, and CH_3OH were all analytical reagent grade, were purified further by freeze–pump–thaw cycles in a vacuum system, vaporized into reservoirs, and mixed with the bath gas Ar before use.

2.2. Identification of CCl_2 radical

In order to affirm that only CCl_2 radicals were detected in the excitation wavelength region in this work, we observed laser-induced fluorescence excitation spectrum of gas-phase CCl_2 produced by dc discharge and cooled in a supersonic free jet. Fig. 2 shows the low resolution LIF spectrum of dichlorocarbene in the 420–600 nm region, which are in good agreement with the low resolution jet fluorescence excitation spectrum of CCl_2 produced by pyrolysis in the 530–555 nm region for both the peak outline and peak positions [24]. Meanwhile, we have determined a higher resolution jet-LIF spectrum, which is identical with a progression of bands of CCl_2 radical in the 497–534 nm region in k-structure resolved [23,25]. It is indicated that we have reliably detected CCl_2 radicals.

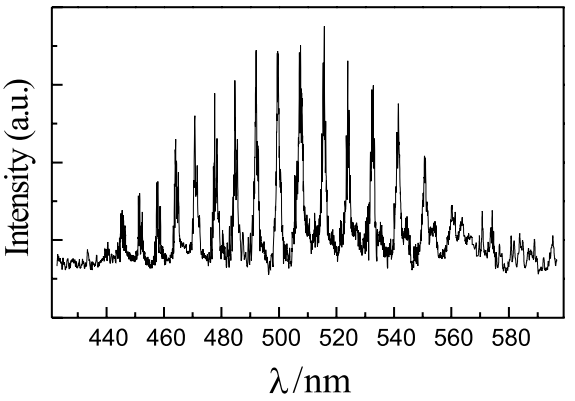

Fig. 2. The low resolution discharge jet fluorescence excitation spectrum of dichlorocarbene in the 420–600 nm region.

3. Description of kinetic three-level model

A typical time-resolved fluorescence decay curve of CCl_2 radical is shown in Fig. 3, in which the quenching process by CH_2Br_2 exists. The decay curve was fitted to

$$y = A_1 \exp(-k_1 t) + A_2 \exp(-k_2 t). \quad (1)$$

It can be seen that the decay curve may be satisfactorily analyzed as a superposition of two lifetime components. In order to contrast, we have measured the time-resolved LIF signal in supersonic free jet conditions, which is shown in Fig. 4. It can be considered that there is no collision between molecules under the supersonic jet conditions. In Fig. 4 it can be seen that it is a mono-exponential decay curve corresponding to the

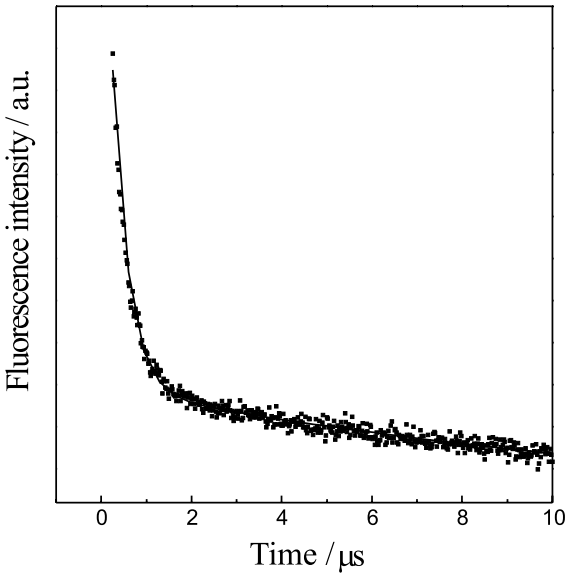

Fig. 3. A typical LIF decay curve of the electronically excited CCl_2 quenched by CH_2Br_2: (■) experiment data and (—) fitting result. Excitation wavelength is 541.52 nm.

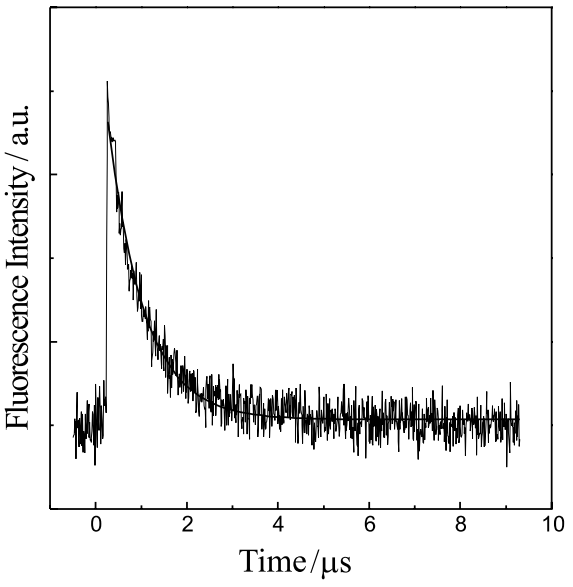

Fig. 4. Time-resolved LIF spectrum of jet-cooled $CCl_2(A\,^1B_1)$. Excitation wavelength is 541.52 nm.

decay of A state. It is indicated that the superposition of two lifetime components is caused by collisions.

Nguyen et al. [35] had calculated the energy levels of CCl_2 radical and found a state $a\,^3B_1$ lies between $A\,^1B_1$ and $X\,^1A_1$. Ibuki [20] speculate that the collision-induced intersystem crossing between the $^1B_1$ and $^3B_1$ states plays an important role in giving rise to the nonexponential behavior. That is, the vibrationally hot $CCl_2(A\,^1B_1)$ radicals produced in the primary excitation process are converted to vibrationally excited CCl_2 in the $^3B_1$ state through bimolecular collisions. Since the phosphorescence lifetime of the $CCl_2(a\,^3B_1 \rightarrow X\,^1A_1)$ transition is expected to be very long, the hot $CCl_2(a\,^3B_1)$ radical would be again quenched to the lower vibrational levels of the $A\,^1B_1$ state. Thus following collisional kinetic mechanism was proposed [31] and shown in Fig. 5.

$$CCl_2(X\,^1A_1) + h\nu \rightarrow CCl_2(A\,^1B_1) \tag{2}$$

$$CCl_2(A\,^1B_1) + Q(M) \overset{k_{q1}(k_{m1})}{\rightarrow} CCl_2(X\,^1A_1) + Q(M) \text{ or other products} \tag{3}$$

$$CCl_2(A\,^1B_1) + Q(M) \overset{\xi_1(\xi_{m1})}{\rightarrow} CCl_2(a\,^3B_1) + Q(M) \tag{4}$$

$$CCl_2(a\,^3B_1) + Q(M) \overset{\xi_2(\xi_{m2})}{\rightarrow} CCl_2(A\,^1B_1) + Q(M) \tag{5}$$

$$CCl_2(a\,^3B_1) + Q(M) \overset{k_{q2}(k_{m2})}{\rightarrow} CCl_2(X\,^1A_1) + Q(M) \text{ or other products} \tag{6}$$

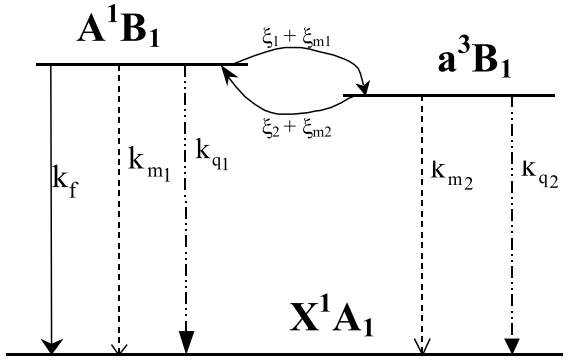

Fig. 5. Diagram of the three-level model of CCl_2.

$$CCl_2(A\,^1B_1) \xrightarrow{k_f} CCl_2(X\,^1A_1) + h\nu_f \quad (7)$$

Q is the quencher. M denotes other molecules (including CCl_4, Ar and the discharge-produced species etc.). The concentrations of M were kept constant in our experiment.

Since what we shall discuss afterwards is a fast pump process (the pulse width of dye laser is 5 ns) and laser intensity is not too high (3–5 mJ/pulse), we assumed the pump and dump would not influence the description of the kinetic behavior after the laser irradiation [36]. Immediately, after laser pulse, it is assumed that the partial densities of CCl_2 (A) and (a) levels are N_A^0 and $N_a^0 = 0$, respectively. k_f represents the Einstein spontaneous emission coefficient from A to X. k_{q1} represents the rate constant of chemical reaction of A state and transition of $A\,^1B_1 \rightarrow X\,^1A_1$ caused by collision with Q. k_{q2} represents the rate constant of chemical reaction and physical quenching of a $^3B_1$. N_q and N_m are the concentration of quencher and M, respectively. k_{mi} ($i = 1$ and 2) represents the collisional removal rate constant by M molecules. ξ_i and ξ_{mi} ($i = 1$ and 2) represent collisional transition rate constants between A and a state with quencher and M.

The kinetic equations of N_A and N_a can be expressed as:

$$\begin{aligned}\frac{dN_A}{dt} &= -k_f N_A - k_{q1} N_q N_A - \xi_1 N_q N_A - k_{m1} N_m N_A \\ &\quad - \xi_{m1} N_m N_A + \xi_2 N_q N_a + \xi_{m2} N_m N_a \\ &= -A N_A + B N_a, \end{aligned} \quad (8)$$

where

$$A = k_f + k_{m1} N_m + \xi_{m1} N_m + k_{q1} N_q + \xi_1 N_q, \quad (9)$$

$$B = \xi_2 N_q + \xi_{m2} N_m, \quad (10)$$

$$\begin{aligned}\frac{dN_a}{dt} &= \xi_1 N_q N_A + \xi_{m1} N_m N_A - \xi_2 N_q N_a \\ &\quad - \xi_{m2} N_m N_a - k_{q2} N_q N_a - k_{m2} N_m N_a \\ &= C N_A - D N_a, \end{aligned} \quad (11)$$

where

$$C = \xi_1 N_q + \xi_{m1} N_m, \quad (12)$$

$$D = \xi_{m2} N_m + k_{m2} N_m + k_{q2} N_q + \xi_2 N_q. \quad (13)$$

Thus, we can arrive at

$$\begin{aligned} N_A &= \frac{1}{\beta - \alpha}\{[(\beta - A)N_A^0 + B N_a^0]e^{-\alpha t} \\ &\quad + [(A - \alpha)N_A^0 - B N_a^0]e^{-\beta t}\}, \end{aligned} \quad (14)$$

$$\begin{aligned} N_a &= \frac{1}{\beta - \alpha}\{[C N_A^0 + (A - \alpha)N_a^0]e^{-\alpha t} \\ &\quad - [C N_A^0 - (\beta - A)N_a^0]e^{-\beta t}\}, \end{aligned} \quad (15)$$

where

$$\alpha + \beta = A + D, \quad \alpha\beta = AD - BC. \quad (16)$$

Noting $N_a^0 = 0$, thus

$$N_A = \frac{1}{\beta - \alpha}\{(\beta - A)N_A^0 e^{-\alpha t} + (A - \alpha)N_A^0 e^{-\beta t}\}, \quad (17)$$

$$N_a = \frac{1}{\beta - \alpha}(C N_A^0 e^{-\alpha t} - C N_A^0 e^{-\beta t}). \quad (18)$$

Since the fluorescence emission of excited CCl_2 radicals is from A state, the detected fluorescence signal intensity is proportional to N_A, i.e.

$$I = \kappa k_f N_A = \frac{\kappa}{\beta - \alpha} N_A^0 k_f [(\beta - A)e^{-\alpha t} + (A - \alpha)e^{-\beta t}], \quad (19)$$

where, κ is the instrument coefficient.

Comparing Eq. (1) with Eq. (19):

$$\alpha = k_1, \quad \beta = k_2, \quad (20)$$

$$A_1 = \frac{\kappa}{\beta - \alpha} N_A^0 k_f (\beta - A), \quad A_2 = \frac{\kappa}{\beta - \alpha} N_A^0 k_f (A - \alpha). \quad (21)$$

Thus,

$$\frac{A_1}{A_2} = \frac{(\beta - A)}{(A - \alpha)}, \quad (22)$$

$$A = \frac{(A_1\alpha + A_2\beta)}{(A_1 + A_2)}, \tag{23}$$

$$D = \alpha + \beta - A. \tag{24}$$

4. Results

Before analyzing the time-resolved signal to derive the fluorescence decay rate constant, a small background, which resulted from the scattered laser irradiation in the reactor without discharge, was subtracted from the gross signal to get a net value. The time-resolved fluorescence net signal of excited CCl_2 radical quenched by CH_2Br_2 and its fitting to two exponential decay curve are illustrated in Fig. 3. A_1, A_2, k_1, and k_2 can be derived by this fitting. A and D can be calculated by Eqs. (23) and (24). The Stern–Volmer plots of A and D vs. $[CH_2Br_2]$ based on Eqs. (9) and (13) are illustrated in Figs. 6 and 7. The slopes of the straight lines are the rate constants $K_A = k_{q1} + \xi_1$ and $K_a = k_{q2} + \xi_2$ of CCl_2 A(0,4,0) and $CCl_2(a\,^3B_1)$ states quenched by CH_2Br_2, respectively. The measured quenching rate constants of the excited CCl_2 radical by methane and substituted methane are listed in Table 1. The uncertainties of K_A and K_a are the standard deviations of the least-squares fitting.

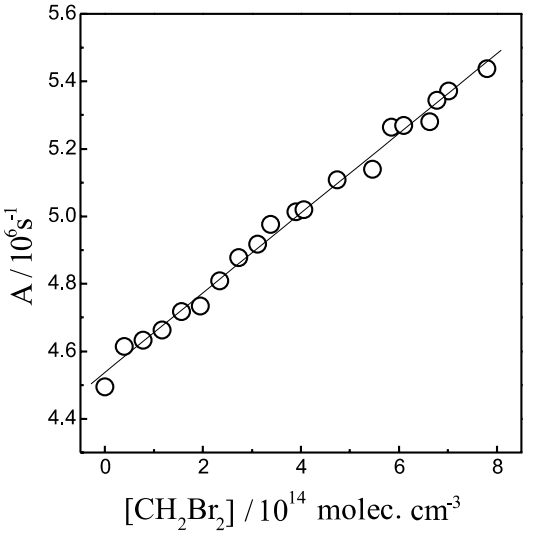

Fig. 6. Plot of A as a function of concentration of CH_2Br_2.

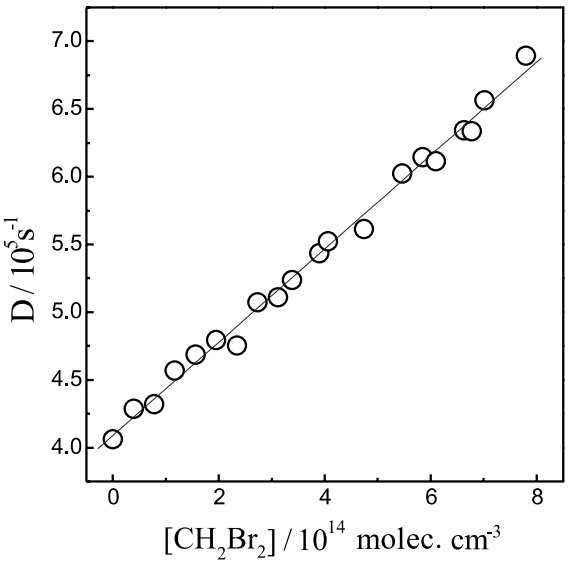

Fig. 7. Plot of D as a function of concentration of CH_2Br_2.

Table 1
Rate constants for collisional quenching of $CCl_2(A\,^1B_1)$ and $(a\,^3B_1)$ by methane and substituted methanes (K_A, K_a are in 10^{-10} cm^3 molecule^{-1} s^{-1}), $T = 290$ K

Quencher	K_A	K_a	Reference
CH_4	1.10 ± 0.11		[26]
CH_4	1.07 ± 0.15	0.43 ± 0.08	This work
CH_3Cl	4.31 ± 0.22	0.93 ± 0.16	This work
CH_2Cl_2	3.99 ± 0.24	0.99 ± 0.17	This work
$CHCl_3$	9.07 ± 0.25	2.35 ± 0.18	This work
CCl_4	5.21 ± 0.19	2.29 ± 0.20	This work
CCl_4[a]	7.47 ± 0.28		[20]
	1.25 ± 0.03		
CCl_4[b]	7.81 ± 0.21		[20]
	0.92 ± 0.02		
CF_4	2.74 ± 0.19	1.02 ± 0.11	This work
CF_2Cl_2	9.09 ± 0.21	2.24 ± 0.10	This work
CH_3NO_3	7.36 ± 0.21	2.19 ± 0.17	This work
CH_2Br_2	11.8 ± 0.27	3.45 ± 0.11	This work
CH_3OH	6.08 ± 0.21	1.04 ± 0.11	This work

[a] Fluorescence at 460 ± 3 nm.
[b] Fluorescence in 500–600 nm region.

5. Discussion

The quenching of the electronically excited CCl_2 radical is a complicated process, including not only physical quenching but also chemical reaction. From Table 1, it is shown that K_A is

higher or much higher than K_a and all bears 10^{-10} $cm^3\,molecule^{-1}\,s^{-1}$ in order of magnitude.

5.1. Collision with CH_4

For CH_4, the value of [26] is the rate constant of CCl_2 A(0,7,0) state and what we measured is the kinetic results of CCl_2 A(0,4,0) state. It is found that our result is in good agreement with that of Ref. [26].

5.2. Collision with CCl_4

The results of Ref. [20] for CCl_4 is included in Table 1, which was obtained by determining the fluorescence decay curve from the photodissociation produced CCl_2 radicals by using a monochromator at 460 ± 3 nm where the emission intensity is the strongest, or through a sharp-cut filter whose transmitting wavelength is longer than 500 nm in 500–600 nm region, because of the weakness of the emission intensity at $\lambda > 500$ nm. They derived two values from the fluorescence decay curve. The K_A and K_a measured by us are in good agreement with the values of Ref. [20] derived from the fast decaying component and the slow decaying component, respectively.

5.3. Comparison of CH_4, CF_4, CCl_4

Because the dipole and quadrupole moments of the three quencher are all zero [37,38], the quenching rate constants of the electronically excited CCl_2 by them are not big and the value for CH_4 is the least and that for CCl_4 is the most one. It indicates the reaction sequence is C–H < C–F < C–Cl bond.

5.4. Collisions with chloromethane molecules

The collision quenching rates of CCl_2 $A\,^1B_1(0,4,0)$ by $CH_{4-n}Cl_n$ ($n = 0$–4) increase with increasing the number of chlorine atoms. It is interesting that the quenching rate of CCl_2 $A\,^1B_1(0,4,0)$ by CCl_4 is somewhat smaller than that by $CHCl_3$. This is probably because the dipole and quadrupole moments of CCl_4 are zero [37, 38]. Therefore, the attractive force between CCl_2 $A\,^1B_1(0,4,0)$ and CCl_4 is smaller than that between CCl_2 $A\,^1B_1(0,4,0)$ and $CHCl_3$ when the CCl_2 $A\,^1B_1(0,4,0)$ radical is close to the collision partners.

5.5. Collisions with CH_2Cl_2, CF_2Cl_2, CH_2Br_2

In the sequence of CH_2Cl_2, CF_2Cl_2, CH_2Br_2 the quenching rate constants K_A and K_a increase steadily. There are same symmetry for the three molecules. It is indicated that CH_2Br_2 is the most reactive one.

5.6. Collisions with CH_3–X molecules

The collision quenching rates of CCl_2 $A\,^1B_1(0,4,0)$ by CH_3–X (X = H, Cl, OH, NO_2) molecules increase in the sequence of –H, –Cl, –OH, $–NO_2$. This is because the volumes of these groups increase gradually. For large molecules, there is a large reaction cross section. Fairchild et al. [39] proposed a theoretical method to calculate the complex formation cross section based on a collisional complex model [40–42]. They have chosen all the attractive forces to construct the effective potential and compute the cross section for complex formation, σ_{cf}, numerically. According to this theory, σ_{cf} is calculated on the basis of a effective potential $V_{eff}(r)$ between collisional partners:

$$V_{eff} = Eb^2/r^2 - C_3/r^3 - C_4/r^4 - C_6/r^6 - C_6'/r^6, \tag{25}$$

where the first term on the right-hand side corresponds to a centrifugal potential, E is the initial kinetic energy at infinite separation, b is the impact parameter, and r is the distance between the mass centers of the CCl_2 radical and the quencher. The C coefficients represent the maxima in the attractive terms due to multiple interactions corresponding to dipole–dipole, dipole–quadrupole, dipole-induced dipole and dispersion forces, respectively. Following this method, we calculated σ_{cf} of $CCl_2(A\,^1B_1)$ with methane and chloromethane molecules. The parameters used in the calculation and calculated complex formation cross sections are summarized in Table 2.

Table 2
Calculated complex formation cross sections σ_{cf} and parameters used in calculation

Quencher	μ[a] (D)	α[a] (10^{-3} nm^3)	Q (10^{-26} esu cm^2)	IP[a] (eV)	σ_{ex} (10^{-2} nm^2)	Calculated σ_{cf} (10^{-2} nm^2)	
						Maximum[b]	Average[c]
CH_4[d]	0.00	2.59	0.00	12.51			90.80[d]
CH_4	0.00	2.59	0.00[e]	12.6	15.75	90.91	90.76
CH_3Cl	1.87	4.72	1.73[f]	11.33	96.73	161.09	116.35
CH_3OH	1.70	3.29	0.50[g]	10.84	116.3	145.3	103.7
CH_3NO_2	3.46	7.37	5.00[g]	11.1	173.7	221.3	143.9
CCl_2	0.48[d]	6.55[d]	0.31[d]	7.95[d]			

[a] Ref. [37].
[b] Calculated using the most favorable orientation method.
[c] Calculated using the averaged orientation method.
[d] Ref. [26].
[e] Ref. [38].
[f] Ref. [44].
[g] Estimated following Refs. [38,43].

According to Ref. [39], the quenching cross section is taken to be proportional to the theoretical cross section for complex formation, $\sigma_Q = P\sigma_{cf}$, where P is the probability that quenching will occur during the residence time of the complex. We have no way of knowing P a priori. Generally, it should be different for different quenchers. The value of P for CH_4 is 0.17 and for CH_3Cl, CH_3OH, CH_3NO_2 are all around 1.0. It appears that the collisional quenching processes of electronically excited CCl_2 radical by CH_3Cl, CH_3OH, CH_3NO_2 is very effective.

Acknowledgements

This work was supported by the National Natural Science Foundation (29973038), the Important Program of the National Natural Science Foundation (10032050) and the National Key Basic Research Special Foundation (G1999075304).

References

[1] J. Hine, J. Am. Chem. Soc. 72 (1950) 2438.
[2] A. Geuther, Ann. Chem. Pharm. 123 (1862) 121.
[3] W.V.E. Doering, A.K. Hoffmann, J. Am. Chem. Soc. 76 (1954) 6162.
[4] R.H. Sherman, R.B. Bernstein, J. Am. Chem. Soc. 73 (1951) 1376.
[5] G.L. Closs, J.J. Coyle, J. Am. Chem. Soc. 87 (1965) 4270.
[6] R.A. Moss, Acc. Chem. Res. 22 (1989) 15.
[7] R.A. Moss, Acc. Chem. Res. 13 (1980) 58.
[8] D.E. Milligan, M.E. Jacox, J. Chem. Phys. 47 (1967) 703.
[9] L. Andrews, J. Chem. Phys. 48 (1968) 979.
[10] M.E. Jacox, D.E. Milligan, J. Chem. Phys. 53 (1970) 2688.
[11] J.S. Shirk, J. Chem. Phys. 55 (1971) 3608.
[12] D.E. Tevault, L. Andrews, J. Mol. Spectrosc. 54 (1975) 110.
[13] V.E. Bondybey, J. Mol. Spectrosc. 64 (1977) 180.
[14] R.E. Huie, N.J.T. Long, B.A. Thrush, Chem. Phys. Lett. 51 (1977) 197.
[15] R. Kiefer, A. Siegel, A. Schultz, Chem. Phys. Lett. 59 (1978) 298.
[16] J.J. Tiee, F.B. Wampler, W.W. Rice, Chem. Phys. Lett. 65 (1979) 425.
[17] J.J. Tiee, F.B. Wampler, W.W. Rice, Chem. Phys. Lett. 73 (1980) 519.
[18] D.J. Clouthier, J. Karolczak, J. Phys. Chem. 93 (1989) 7542.
[19] D.A. Predmore, A.M. Murray, M.D. Harmony, Chem. Phys. Lett. 110 (1984) 173.
[20] T. Ibuki, N. Takahashi, A. Hiraya, K. Shobatake, J. Chem. Phys. 85 (1986) 5717.
[21] T. Ibuki, A. Hiraya, K. Shobatake, Chem. Phys. Lett. 157 (1989) 521.
[22] M. Fujitake, E. Hirota, J. Chem. Phys. 91 (1989) 3426.
[23] J.I. Choe, S.R. Tanner, M.D. Harmony, J. Mol. Spectrosc. 138 (1989) 319.
[24] D.J. Clouthier, J. Karolczak, J. Chem. Phys. 94 (1991) 1.
[25] Q. Lu, Y. Chen, D. Wang, Y. Zhang, S. Yu, C. Chen, M. Koshi, H. Matsui, S. Koda, X. Ma, Chem. Phys. Lett. 178 (1991) 517.
[26] I. Merelas, J.A. Fernández, P. Puyuelo, M.N. Sánchez Rayo, D. Husain, F. Castaño, Chem. Phys. 254 (2000) 77.
[27] G. Smolinsky, R.A. Gottscho, S.M. Abys, J. Appl. Phys. 54 (1983) 3518.

[28] J. Tokuda, M. Takai, H. Nakai, K. Gamo, S. Namba, J. Opt. Soc. Am. B 4 (1987) 267.
[29] T. Yamamoto, N. Ootsuka, J. Nucl. Sci. Technol. 18 (1981) 913.
[30] M. Wagner, Ber.-Max.-Planck-Inst. Stoemungsforsch. 4 (1996) 76–82.
[31] Y. Gao, Y. Chen, X. Ma, C. Chen, Chem. Phys. Lett. 339 (2001) 209.
[32] C. Chen, X. Wang, S. Yu, Q. Lu, X. Ma, Chem. Phys. Lett. 197 (1992) 286.
[33] C. Chen, F. Wang, Y. Chen, X. Ma, Chem. Phys. 230 (1998) 317.
[34] C. Chen, Q. Ran, S. Yu, X. Ma, J. Chem. Phys. 99 (1993) 1070.
[35] M.T. Nguyen, M.C. Kerins, A.F. Hegarty, N.J. Fitzpatrick, Chem. Phys. Lett. 117 (1985) 295.
[36] X. Ma, F. Kong, Laser Chemistry, University of Science and Technology of China Press, Hefei, 1990.
[37] D.R. Lide, CRC Handbook of Chemistry and Physics, 71st ed., CRC press, Florida, 1991.
[38] D.E. Stogryn, A.P. Stogryn, Mol. Phys. 11 (1966) 371.
[39] P.W. Fairchild, G.P. Smith, D.R. Crosley, J. Chem. Phys. 79 (1983) 1795.
[40] J.C. Tully, J. Chem. Phys. 61 (1974) 61.
[41] G.E. Zahr, R.K. Preston, W.H. Miller, J. Chem. Phys. 62 (1975) 1127.
[42] D.L. Holtermann, E.K.C. Lee, R. Nanes, J. Chem. Phys. 77 (1982) 5327.
[43] R.A. Copeland, M.J. Dyer, D.R. Crosley, J. Chem. Phys. 82 (1985) 4022.
[44] D.L. Vanderhart, W.H. Flygare, Mol. Phys. 18 (1970) 77.